On the Charged Particle Drag acting on LAGEOS

J. I. Andrés[(a)] J.R. Sanmartín[(b)]

R. Noomen[(a)]

[(a)] Delft Institute for Earth Observation and Space Systems, DEOS
Delft University of Technology

[(b)] Departamento de Física, E.T.S.I. Aeronáuticos, Universidad Politécnica

2007

Abstract

A recent study by the authors points to Charged Particle Drag (CPD) as a contributor to revisit in the LAGEOS non-gravitational perturbations problem. Such perturbations must account for dynamical contributions in the order of pms^{-2} . The simulated effect takes into account: *(i)* spatial and temporal variations of the plasmatic parameters (temperature and concentration of the species), *(ii)* spacecraft potential variations caused by both the eclipse passages and variations in the parameters mentioned above, and *(iii)* solar and geomagnetic conditions. Furthermore, recent theoretical improvements concerning scattering drag overcome previous limitations allowing for a complete formulation of this effect.
For each satellite the lifetime CPD instantaneous acceleration is computed. The plasmatic parameters have been obtained from the Sheffield Coupled Thermosphere-Ionosphere-Plasmasphere (SCTIP) semi-empirical model (up to the polar region), as well as analytical/empirical approximations based on spacecraft measurements for the auroral and polar regions. Results show that maximum amplitudes for LAGEOS-I are larger than those for LAGEOS-II: -85 pms^{-2} and -70 pms^{-2} respectively. This is due to the almost (magnetically) polar orbit configuration of the first, producing larger combinations of plasmatic parameter values. High solar activity has a huge impact in the resulting LAGEOS accelerations: it yields a perfect modulation of the resulting acceleration with maximum amplitudes up to a factor of 10 when comparing low and high activity periods. On the other hand, the impact of the geomagnetic activity results into a reduction of the effect itself, probably due to a decrease in the hydrogen concentration for high energy input periods. The acceleration results will be used in a refined orbit computation in a subsequent investigation.

1 Introduction

With a spherical shape, a low area-to-mass ratio in order to diminish surface forces, and 426 retroreflectors studded over their surface for the purpose of facilitating Satellite Laser Ranging (SLR) measurements, for very accurate satellite orbit computations, the satellites LAGEOS-I and II have proven an essential tool in geophysics since their launch on 4 May, 1976 and 22 October, 1992 respectively. The unprecedented accuracy of the SLR observations, orbit solutions, and derivatives, make LAGEOS a unique contributor for quantifying geophysical phenomena, its accuracty being directly related to that of the reconstructed orbits.

For the aforementioned reasons and due to an intriguing along-track deceleration which causes the decay of the semimajor axis of the orbit at a rate of approximately 1.1 mmd^{-1} [*Smith and Dunn*, 1980], their orbits have been intensively studied since the early 1980s. A number of publications has been dedicated to investigate various physical effects as the possible cause of such a decay: thermal (re)radiation, solar and terrestrial radiation, neutral and charged particle drag, etc. A very interesting feature shown in the empirical accelerations obtained in the orbit determination process is the eclipse modulation of the signal. This can be related to a number of factors: changes in radiation inputs, environmental and satellite properties, physical magnitudes, etc. Fruit of a thorough thermal study, *Andrés et al.* [2006] suggest that CPD might be an important contributor to revisit in order to explain such a feature.

For a typical orbital revolution, while in eclipse conditions, the satellite will be utterly non-illuminated, whereas for non-eclipse conditions, half of it will be facing the Sun (sunlit part), whereas the other half will be shaded (shadow part). For the former (eclipse) conditions, the satellite will reach a charging equilibrium with its surroundings by balancing the thermal ion electron collection. On the other hand, for non-eclipse conditions, photons impinging into the sunlit part, will result into an emission of photoelectrons from said surface, with the consequent modification of the spacecraft charging potential. Therefore the floating potential will be different under eclipse and non-eclipse conditions. Similarly, the plasmasphere receives a radiation input modulated by the eclipse geometry. This input is associated to chemical and energy reactions, determining the local dynamics of the different species involved in the diffusion and chemical equilibria, and consequently, temperature and density distribution. The temporal and spatial variability of said parameters do leave an imprint on the satellite dynamics.

At least four limitations can be identified in previous LAGEOS CPD studies: *(i)* the use of a fluid dynamics expression for the CPD [*Rubincam*, 1980], which exclusively depends upon the orbital velocity squared of the satellite v_{orb}^2 without taking into account the ion thermal speed and the spacecraft

potential, *(ii)* the use of a first approximation in evaluating the drag coefficient C_D for the latter fluid dynamics expression [*Rubincam*, 1980; *Afonso et al.*, 1985], *(iii)* the use of approximations for the drag due to scattering of the particles as an empirical expression, or as a percentage of the direct collision drag [*Rubincam*, 1980; *Afonso et al.*, 1985; *Pitts and Knechtel*, 1965], and *(iv)* the use of wrong assumptions about the ion distribution around the spacecraft, leading to wrong calculations based upon a chosen (*e.g.,* screened Coulomb) potential behaviour [*Afonso et al.*, 1985]. Other studies only included estimations of the effects based upon a cylindrical geometry approximation, *e.g.,* [*Afonso et al.*, 1980] based upon [*Fournier*, 1971], or built up results based upon previous authors, *e.g.,* [*Rubincam*, 1990; *Barlier et al.*, 1986]. Besides, due to the uncertainty and scarcity of the available plasmatic data at that time, these studies could only provide a constant (averaged) along-track deceleration of about 2 pms^{-2}; as a result, no spatial or temporal variation via the (plasmatic) parameters involved in the calculations was allowed for. It can be concluded therefore, that a more detailed analysis of the problem is required.

In spite of theoretical and practical limitations at the early days of development, the two main CPD contributors were identified correctly: drag due to direct collisions and drag due to the scattering of the impinging particles (*e.g.* [*Brundin*, 1963]). Recently, a series of dedicated articles from *Hutchinson* [2002, 2003, 2005, 2006] have presented a numerical and theoretical anlysis for an arbitrary ratio between satellite orbital and ion thermal speed allowing for the detailed formulation of the scattering theory for the parameter domain at LAGEOS conditions.

The present study addresses the aforementioned issues and give more insight into the LAGEOS CPD problem by means of a complete model. For this, more light is shed over the LAGEOS parameter domain and MEO orbits specific conditions. This will be followed by the theoretical formulation of the effects considered. Then, modelled results will be presented for both LAGEOS-I and -II using semi-empirical plasmaspheric data (T_e, T_i, n_e, and n_i) for the aforementioned plasmatic parameters from SCTIP, a plasmasphere semi-empirical model, and other empirical approximations for higher latitudes. Finally, conclusions will be drawn and recommendations for future studies and/or missions will be given.

2 Plasmatic environment

The complex physical structure of the plasmasphere is driven by a number of diffusion and magnetic processes [*Ganguli et al.*, 2000]. A characterisation of the different conditions is generally given in terms of the following parameters: local times (solar or magnetic, LST and MLT respectively), the McIlwain parameter $L = \varrho/\cos^2\alpha$ [*McIlwain*, 1961], with $\varrho = r/r_\oplus$ the

dimensionless distance in Earth radii and α the geomagnetic (dipolar) latitude, the geomagnetic activity (usually given in literature by A_p and K_p indices), the solar activity as given by the integrated emission from the solar disc at 2800 MHz, *i.e.,* the radio flux at 10.7 cm wavelength (expressed in solar flux units, $1\ \mathrm{sfu} = 10^{-22}$ Wm^{-2}Hz^{-1}), hemisphere, and atmospheric composition.

At approximately 5900 km altitude, the LAGEOS satellites move through the plasmasphere and the polar regions, thus encountering very different conditions. The magnetic field lines are closed and resemble those from a dipole in the plasmaspheres, and are effectively open in the polar regions. The McIlwain parameter varies from $L \simeq 1.9$ over the magnetic equator, to large values close to the poles for LAGEOS-I, and with smaller values for LAGEOS-II due to the lower inclination of the orbit ($i_{\mathrm{L-I}} = 109^\circ$ *vs.* $i_{\mathrm{L-II}} = 52^\circ$). Variations of the latter parameters modify the diffusion and magnetic processes yielding the composition, concentration and temperature of the species.

The thermal structure of the plasmasphere is closely related to the density structure, and significantly affects the composition of the plasma [*Comfort*, 1996]. Data on this have been obtained by a number of missions since the 1960s, *e.g.,* OGO, Alouette, Prognoz, ISIS, AE, DE, and EXOS-D (latter on renamed as Akebono). In paralllel, empirical plasmaspheric models have been developed based on finetuning of theoretical models with empirical data, *e.g.,* CTIP [*Millward et al.*, 1996].

As for the magnetic poles and auroral zones, calculation of the plasmatic parameters for the open flux tubes is very much dependent on the boundary conditions imposed at higher altitudes, which in turn strongly depend on the geomagnetic conditions, therefore the accuracy of the results is very much diminished (Dr. R. Balthazor, personal communication). Despite their importance in auroral acceleration theories and polar ion outflow, these zones are poorly characterised in terms of the background plasma temperature [*Kletzing et al.*, 1998]. On the contrary, the density parameter is in a better situation due to a strong interest in characterising: *(i)* the experimentally found (intense, nonlinear) electric field structures on auroral field lines at altitudes of 1 R_E (*e.g.,* [*Johnson et al.*, 2001] and references therein), and *(ii)* the flows of light and heavy ions in the auroral and polar zones, especially the dynamics of the so-called cleft ion fountain ([*Tu et al.*, 2005] and references therein). Said electric field structures can accelerate electron beams outwards, or inwards provoking aurora. In general, data at this (LAGEOS) altitude have been obtained by a number of missions: S3-3, DE-1, and Viking.

Symbol	Name	Value	Units
a	Semimajor axis	12270×10^3	m
r_s	Satellite radius	0.3	m
λ_D	Debye length	0.136	m
v_{th_i}	Ion thermal speed	9.8×10^3	m s^{-1}
v_2	Orbital speed	5.7×10^3	m s^{-1}
n_e	Typical electron density at MEO	3×10^9	m^{-3}
$k\,T_e$	Electron temperature	0.5^1	eV
J_{th_e}	Thermal electron current density	$\simeq 50 \times 10^{-6}$	A m^{-2}
J_{th_i}	Thermal ion current density	1.16×10^{-6}	A m^{-2}
J_{ph_0}	Photoelectron emission density of Al @ 1AU	120×10^{-6}	A m^{-2}

[a] Equivalent to approximately 5800 K.

Table 1: Nominal parameter values involved in the description of the photoelectric emission effect.

3 The LAGEOS parameter domain

Contrary to the LEO case, for LAGEOS altitudes the photoelectric emission effect is the driving potential effect. In addition, the conductive properties of LAGEOS differ from those of typical GEO satellites (with large dielectric surfaces like solar panels coating). As a result, no potential barrier phenomenon exists, for no dielectric material causes the accumulation of charge over the surface nor the consequent dipole formation (due to large potential differences between satellite shadow and sunlit parts), and thus the current equilibrium happens locally. On the contrary, the rapid conduction process causes *(i)* the spacecraft potential distribution to be uniform as a first approximation, *i.e.,* it behaves as a monopole (see [*Andres*, 2007]), and *(ii)* the current equilibrium to be global.
The dynamical interaction between a conductor (charged or not) and a surrounding plasma depends upon several ratios and physical parameters, namely *(i)* the satellite's orbital speed to ion thermal speed, *(ii)* the Debye length and a satellite characteristic radial dimension r_s, and *(iii)* the thermal (ion and electron) and photoelectron currents and ratios amongst them. These will be treated in the following subsections. Values of these parameters are given for the chosen nominal conditions (*cf.* Table 1), namely a proton H^+ environment. Albeit that for the majority of the situations, protons are indeed the major constituent, for large values for the energy inputs as well as for certain spatial locations (auroral zones and the associated plasma fountain), O^+ can become as abundant as H^+. These situations are considered as punctual and neglected altogether. By doing so, the conservative solution is chosen, since the larger atomic mass of O^+ would result into larger disturbances. Expected deviations from the nominal val-

ues presented in Table 1 are expressed here in the form of scaling variables: $\tilde{\mathcal{T}} = \frac{T}{T_0}$, $\tilde{n} = \frac{n}{n_0}$ and $\tilde{\mathcal{J}}_{ph} = \frac{J_{ph}}{J_{ph_0}}$.

3.1 Velocity ratios

The ratio between the satellite orbital speed and the ion thermal speed determines the type of flow regime that the spacecraft encounter. The LAGEOS orbital velocity can be readily calculated, assuming the orbits to be circular, which is an excellent approximation since the eccentricities are very small (*cf.* Table 1). This yields $v_{orb} = \sqrt{\mu/a} \simeq 5.7$ kms^{-1} (*cf.* Table 1). As for the ion thermal speed, this depends upon the ion temperature T_i (a very good approximation consists of taken this equal to that of the electrons T_e):

$$v_{th_i} = \sqrt{2kT/m_i} \simeq 9.8\,\tilde{T}^{1/2}\,\mathrm{kms}^{-1} \tag{1}$$

where k is the Boltzmann constant, and m_i the ion mass; the numerical value is given for the proton H^+ case, for this is the major constituent at LAGEOS altitude. This yields a value for the thermal ion speed of about two times the orbital speed, hence the dimensionless speed

$$u = \left(\frac{v_{orb}}{v_{th_i}}\right) \simeq 0.5$$

which makes *(i)* the regime subsonic, and *(ii)* the ion distribution function reasonably isotropic.

3.2 Electrostatic shielding ratios

For finite-size conductors, the ratio between the the Debye length λ_D and the satellite radius r_s:

$$\bar{\lambda}_D = \left(\frac{\lambda_D}{r_s}\right)$$

provides an estimation of the importance of screening. For the aforementioned values the Debye length equals to (value in meters):

$$\lambda_D \simeq 0.136\,\tilde{n}^{-1/2}\,\tilde{T}^{1/2} \tag{2}$$

hence $\bar{\lambda}_D \simeq 0.45\,\tilde{n}^{-1/2}\,\tilde{T}^{1/2}$. For nominal conditions, the aforementioned ratio is less than unity, which has significant implications for the structure of the potential around the satellite as will be discussed in Section 5.

4 Floating potential

The current equilibrium condition yielding the floating potential value ϕ_p, greatly differs for non-eclipse and eclipse conditions, as indicated previously.
For the latter condition the floating potential is usually negative and the current equilibrium, *i.e.,* thermal electron current balancing thermal ion current, can be written as:

$$J_{th_e} \exp(\psi_p) = J_{th_e} \sqrt{\frac{T_i}{T_e}} \sqrt{\frac{m_e}{m_i}}\, j\left(\bar{\lambda}_D, \psi_p\right) \tag{3}$$

where $j(\bar{\lambda}_D, \psi_p)$ is a tabulated function of the inverse of the aforementioned parameter $\bar{\lambda}_D$ and the dimensionless potential $\psi_p = e\phi_p/kT_e$, taken from Langmuir probes ([*Laframboise*, 1966, Figure 20], for equal temperature of the species, *i.e.*, $T = T_e = T_i$). Taking natural logarithms in the expression above yields:

$$\psi_p = (-3.76 + \ln j) \tag{4}$$

As an estimation, for the aforementioned nominal parameters $\ln j$ is approximately equal to unity and therefore $\psi_p \simeq -2$. In order to solve this equation, an iteration procedure is combined with tabulated j values to obtain ψ_p. However, the latter equation is mainly driven by the $\frac{1}{2}\ln\left(\frac{m_e}{m_i}\right) = -3.76$ term, since $j \simeq \mathcal{O}(1)$.
When not in eclipse, the floating potential can be still considered as nearly uniform, *i.e.,* behaving as a monopole: variations of the potential inside the spacecraft $\Delta\phi$ being $\ll \phi$. Therefore, under the assumption of a small positive constant floating potential, [*Laframboise*, 1966, Figure 20] suggests that the Orbital Motion Limited (OML) theory, *e.g.,* [*Hutchinson*, 1987] applies. A current balance for the entire spacecraft as shown in Figure **??**, yields:

$$4\pi r_s^2 J_{th_e}(1 + \psi_p) = \pi r_s^2 J_{ph} \tag{5}$$

Note that in the case of the photoelectron current, due to its directionality, only the cross sectional area appears in the expression. Furthermore, on the basis of $\psi_p \simeq 0^{\pm}$ the ion thermal currents are neglected since the ratio $J_{th_i}/J_{th_e} \ll 1$. Another immediate consequence is that regardless of its sign, Equation 5 is valid for both hemispaces $\psi_p > 0$, $\psi_p < 0$: for the former the formulation is exact under the OML theory, and for the latter the exponential can be approximated by its Taylor's expansion for $|\psi_p| \simeq 0$, thus obtaining the expression in Equation 5 again, thus ensuring its consistency.
For the chosen 'nominal conditions', and approximating the term $(1 + \psi_p)$ by the exponential, the thermal electron current density can be written as

$J_{th_e} \simeq 50\,\tilde{n}\,\tilde{T}^{1/2}\,\mu A\,m^{-2}$ (*cf.* Table 1), which yields a value for the floating potential of

$$\exp\left(-|\psi_p|\right) \simeq 1.67\,\tilde{n}\,\tilde{T}^{1/2}\,\tilde{\mathcal{J}}_{ph}^{-1} \tag{6}$$

which results into the following expression for the potential:

$$|\psi_p| = -\left(0.51 + \ln\tilde{n} + \frac{1}{2}\ln\tilde{\mathcal{T}} - \ln\tilde{\mathcal{J}}_{ph}\right) \tag{7}$$

With the floating potential value expressed in terms of variables of the problem, the drag forces can now be calculated.

5 Formulation

In addition to the classical direct collision in neutral particle drag, Coulomb drag, *i.e.*, deflection of an incoming particle due to long range Coulomb forces, also exists. The ion flow in the parametric domain of interest being subsonic makes the analysis of the forces more simple. Other possible contributors such as wave drag are not present here since the characteristic times of the problem show that it can be considered as electrostatic, *i.e.*, stationary.

5.1 Direct collision

Recently, *Hutchinson* [2005] has suggested a way of calculating the direct collision force by taking the OML momentum flux rate integrated over a shifted Maxwellian velocity distribution (see also [*Uglov and Gnedovets*, 1991]), under the OML assumptions of *(i)* a spherically symmetric potential and *(ii)* no potential barrier. His result is here rewritten in the following way:

$$\frac{F_c}{nkT_i\,\mathcal{A}_\varnothing} = \mathcal{P}(u) + \mathcal{Q}(u)|\psi_p| \tag{8}$$

where $n\,kT_i$ the thermal pressure exerted by the proton flux, $u = u_2$ the dimensionless speed of the test particle (*i.e.*, LAGEOS), and the functions $\mathcal{P}(u)$ and $\mathcal{Q}(u)$ are:

$$\begin{aligned}\mathcal{P}(u) =& \frac{u(1+2u^2)\exp\left(-u^2\right) + \frac{\sqrt{\pi}}{2}\left[4u^4+4u^2-1\right]\mathrm{erf}(u)}{\sqrt{\pi}\,u^2}\\ \mathcal{Q}(u) =& \frac{2u\exp\left(-u^2\right) - \sqrt{\pi}(1-2u^2)\,\mathrm{erf}(u)}{\sqrt{\pi}\,u^2}\end{aligned} \tag{9}$$

with $\mathrm{erf}(u)$ the error function. In this manner, the linear dependency of the collision drag on the floating potential is clearly exhibited.

5.2 Scattering

The OML assumptions of conservation of energy and angular momentum can be used to obtain the scattering section σ_s, and therefore the exchange of momentum between the test particle (spacecraft) and the incoming particles as (after [*Hutchinson*, 1987]):

$$\mathbf{F}_o = \int m_r \mathbf{v}_1 \; v_1 \; \mathcal{F}_i(\mathbf{v}_1, \mathbf{v}_2) \, \sigma_s(v_1) \, d\mathbf{v}_1^3 \tag{10}$$

with m_r the reduced mass, which can be approximated by that of the ions $m_r \simeq m_i$ since $m_{\text{LAGEOS-I}} \gg m_i$, $m_r \mathbf{v}_1$ the linear momentum of the incoming ions, $\mathcal{F}_i(\mathbf{v}_1, \mathbf{v}_2)$ their drifted Maxwellian distribution, and $\sigma_s(v_1)$ the scattering section w.r.t. the ions. In order to integrate the momentum exchange from the hyperbolic orbits to the test particle as given by Equation 10, one necessitates the form of the potential in the vicinity of the satellite.
Typically, an analytical expression for this integral has been obtained in previous studies by assuming that *(i)* only those ions approaching sufficiently close to the test particle contribute to the momentum transfer, and *(ii)* the potential form corresponds to a screened Coulomb form within a few Debye lengths from the particle and to an inverse square one beyond that, *e.g.*, [*Daugherty et al.*, 1992; *Khrapak et al.*, 2002]. This leads to an expression depending on the Coulomb logarithm, expressed in terms of a minimum and a maximum impact parameter. These parameters are usually taken as $b_{min} = b_{90}$, the impact parameter for 90° scattering in the center of mass frame, and $b_{max} = \lambda_D$, the Debye length. For values of the Debye length in the order of the test particle radius, as is the case for LAGEOS, incoming ions do penetrate the Debye sphere, therefore taking the b_{max} cutoff implies neglecting a significant part of the ion momentum transfer [*Khrapak et al.*, 2002].
At difference with a strictly point charge however, a finite body, *i.e.*, LAGEOS, behaves as a sink of charges. The way in which the potential and density approach their undisturbed values depend then separately both on the Debye length and on the body characteristic length. In the case of the repelled species, *Lam* [1965] showed how the finite body (sink) effect affects the density profile independently of screening. Thus for LAGEOS, the form of the potential around the spacecraft does fit an unscreened Coulomb or a Debye-Huckel form worse than an inverse square law $\phi \sim \phi_p r_s^2 / r^2$.
Based on this form of the potential, the scattering force integral can be written as, a detailed analysis leads to [*Andres*, 2007] (recall $u = u_2$):

$$\frac{F_o}{nkT_i \, \mathcal{A}_\varnothing} = \mathcal{G}(u, |\psi_p|) \, \psi_p^2 \tag{11}$$

where the function $\mathcal{G}(u, |\psi_p|)$ is given by:

$$\begin{aligned}\mathcal{G}(u,|\psi_p|) =& \mathcal{C}\left\{\frac{1}{au^2}\left[1-\exp\left(-\frac{u^2}{2}\right)+u\sqrt{\frac{\pi}{2}}\left(1-\mathrm{erf}\left(u\right)\right)\right]+\right.\\ &+\int_0^\infty f(u,w_r,|\psi_p|)\arctan\left(\tilde{D}|(u-w_r)|\sqrt{|\psi_p|}\right)dw_r+\\ &\left.-\int_0^\infty f(u,w_r,|\psi_p|)\arctan\left(\tilde{D}(w_r+u)\sqrt{|\psi_p|}\right)dw_r\right\}\end{aligned} \tag{12}$$

with a, h_∞, $\mathcal{C}$, and $\tilde{D}$, constants ($a = 4.22$, $h_\infty = \pi^2/8$, $\mathcal{C} = 4(2\pi)^{-1/2}\, a\, h_\infty \simeq 8.31$, $\tilde{D} = \sqrt{a/2h_\infty} \simeq 1.71$). with $f(u, v, |\psi_p|)$ given by:

$$f(u,w_r,|\psi_p|) = \exp\left(-\frac{w_r^2}{2}\right)\frac{\tilde{D}^2(u^2-w_r^2)-|\psi_p|}{2au\tilde{D}}|\psi_p|^{-1/2} \tag{13}$$

which can then be calculated numerically (see Figure 1). Note that when $u_2 \to 0$, $F_0 \to 0$, which is to be expected due to the spherical symmetry of the function in the integrand if $u_2 = 0$. On the other hand, for $|\psi_p| \to 0$, $F_0 \to 0$ for no scattering force occurs if the satellite is not charged.

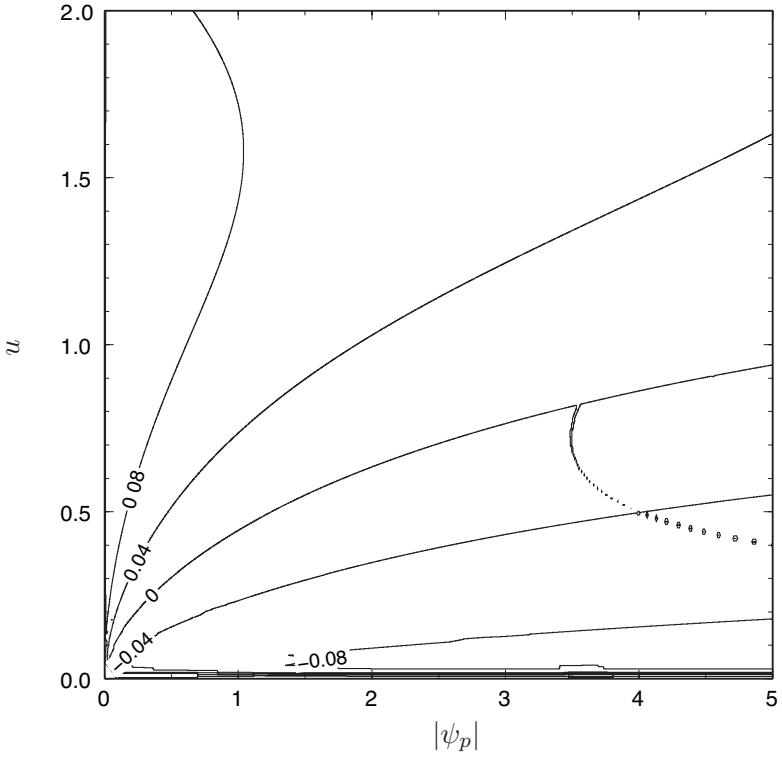

Figure 1: Contour values of the numerically computed $\mathcal{G}(u, |\psi_p|)$ function.

5.3 Total force

Summarising, the total (dimensionless) force (subindex t), summation of Equations 8 and 11, can be conveniently written as an expansion of the dimensionless potential $|\psi_p|$

$$\frac{F_t}{nkT_i\,\mathcal{A}} = \mathcal{P}(u)\left[1 + \mathcal{Q}^*(u)\,|\psi_p| + \mathcal{G}^*(u, |\psi_p|)\,\psi_p^2\right] \tag{14}$$

where $\mathcal{Q}^* = \mathcal{Q}/\mathcal{P}$ and $\mathcal{G}^* = \mathcal{G}/\mathcal{P}$.
The analytical functions $\mathcal{P}(u)$, $\mathcal{Q}(u)$, and $\mathcal{Q}^*(u)$ are depicted in Figure 2. An interesting feature of the latter function is its (almost) constant value for the range of normalized velocities considered $u \in [0, 1]$.

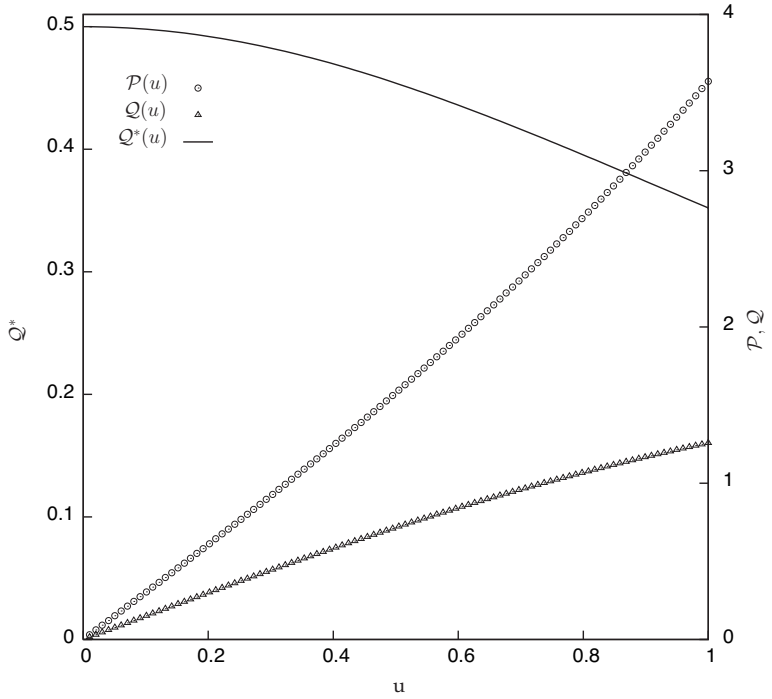

Figure 2: Analytic functions $\mathcal{P}(u)$, $\mathcal{Q}(u)$ and $\mathcal{Q}^*(u)$. The first two functions are depicted using the bottom and right axes, whereas the latter one is depicted using the bottom and left axes.

6 Plasmaspheric data

As a result of the availability of the data, two types of data have to be combined to obtain a global coverage for both temperature and density:

(i) numerical data for low and mid magnetic latitudes as given by semi-empirical models. For this purpose, SCTIP a three dimensional, fully coupled, numerical model of the thermosphere, low latitude plasmasphere and high latitude ionosphere is used. SCTIP is based upon solving the equations of continuity, momentum and energy balance, together with equilibrium reactions for the different constituents considered. As a result, SCTIP provides concentrations and temperatures for ions (H^+ and O^+) and electrons, as well as velocities along the magnetic field lines for these ions, with a very good confidence in regions bounded by magnetic latitudes of approximately $\pm 45^\circ$ [*Millward et al.*, 1996], and with less confidence for upper latitudes (R. Balthazor, private communication). Thus no SCTIP data have been used over the polar or auroral regions. Considering the inclination of the Earth's magnetic dipole $\mathcal{D} \simeq 11^\circ$, and the inclination of the satellites, it turns out that the LAGEOS-II orbit is included in a region bounded by magnetic latitudes of approximately $\pm 65^\circ$, *i.e.*, reaching auroral zones, whereas LAGEOS-I traverses all regions, thus including the auroral and the polar zones.

(ii) truly empirical: either direct measurements or empirical approximations of the latter. For the auroral and polar regions, temperature values as given in *Kletzing et al.* [1998, Figure 6] is used (see Table 2). The uncertainties in these data are caused by the binning procedure, which accounts only for MLT and Invariant Latitude (ILAT), thus encompassing very different solar and geomagnetic conditions. Although no values are provided at LAGEOS altitude exactly, extrapolation has been used, for which typical uncertainty values for ILAT$\in [65^\circ, 80^\circ]$ are within $[0.3, 1.0]$ eV, the minimum happening for MLT$\in [21:00, 24:00]$, and the maximum uncertainty for the morning sector. The polar regions show interpolated uncertainties of $[0.75]$ eV, or 40% of the observation. As regards the electron density, this will be taken from the empirical model presented in *Nsumei et al.* [2003, Equation 2b]. Their Figure 4 show an average electron density distribution w.r.t. altitude, which for $r \simeq 2R_\oplus$ depicts an uncertainty of about 18% of the mean. Again, these values are understood as average over very different solar and magnetic conditions.

Conjugation of both types of data is done via Delauney triangulation. The [*Watson*, 1982] triangulation algorithms has been preferred over others for its faster while accurate results.

7 Accelerations

Time series of accelerations have been obtained for both LAGEOS-I and II from their respective launches until mid 2006, at every time step ($\tau_{\text{step}} =$

	MLT [h]							
Region[1]	[0 : 3]	[3 : 6]	[6 : 9]	[9 : 12]	[12 : 15]	[15 : 18]	[18 : 21]	[21 : 24]
Auroral[2]	0.75 [3]	1.0 [3]	-	1.0	1.0 [3]	-	1.0	0.75
Polar					1.75			

[a] Auroral zone bounded by ILAT $\in [65^\circ, 80^\circ]$ and polar region as ILAT $> 80^\circ$.
[b] Missing zones have been dealt with via interpolation through arctg functions.
[c] Symmetry w.r.t. 0 h MLT applied.

Table 2: Empirical values for auroral and polar regions as reported in *Kletzing et al.* [1998, Figure 6] after applying symmetry w.r.t. the 0 h MLT. All values given in eV.

60 s), as to capture eclipse passages and spatial variations of the plasmatic parameters. The results (expressed in the usual three in-orbit components), together with the satellite floating potential ϕ_p, are depicted in Figures 3 and 4, for LAGEOS-I and LAGEOS-II, respectively. Due to the large size of the data files, results have been plotted every 180 steps of integration, *i.e.,* once every 1.5 h, (a comparison with the original results showed that no aliasing effect is introduced in the representation here). Both figures show the solar and geomagnetic indices together with the ideal shadow function, so as to illustrate the correlation between these parameters and the physical effect. This can be clearly seen in both figures, especially for the LAGEOS-I case, for which the effect of the three solar cycles undergone during its lifetime, as well as the eclipse passages, cause a clear modulation on the resulting CPD acceleration (*cf.* the along-track component in Figure 3): it increases with solar activity as reported in [*Barlier et al.*, 1986]. The variations in the accelerations can be explained by changes in the plasmatic parameters caused by both spatial effects (the eclipse modulation) and variations in energy input (the Schwabe-Wolf cycle), which modify the ion thermal pressure as well as (the formulation of and thus) the floating potential of the spacecraft (*cf.* Equations 4 and 7). Inspection of the magnitude of these accelerations in Figures 3 and 4 shows that it can reach instantaneous values of 85 and 70 pms^{-2} for LAGEOS-I and LAGEOS-II respectively. This is most likely caused by the inclination of the orbit, which takes LAGEOS-I over the polar and auroral zones, for which the temperature values are higher than in the equatorial and mid latitude zones (recall that LAGEOS-II stays within the magnetic parallels at $\pm 60^\circ$ approximately). The other two components of the total acceleration (radial and out of plane) do also exhibit a modulation w.r.t. the $F_{10.7}$ index and eclipse passages, as expected, yet their values are a mere 5% of those for the along-track component. For a perfectly circular orbit with no ion drift velocity, these should be equal to zero, since by definition the drag is antiparallel to the relative velocity, yet the small eccentricity of the orbit and the osculating values provided by GEODYN,

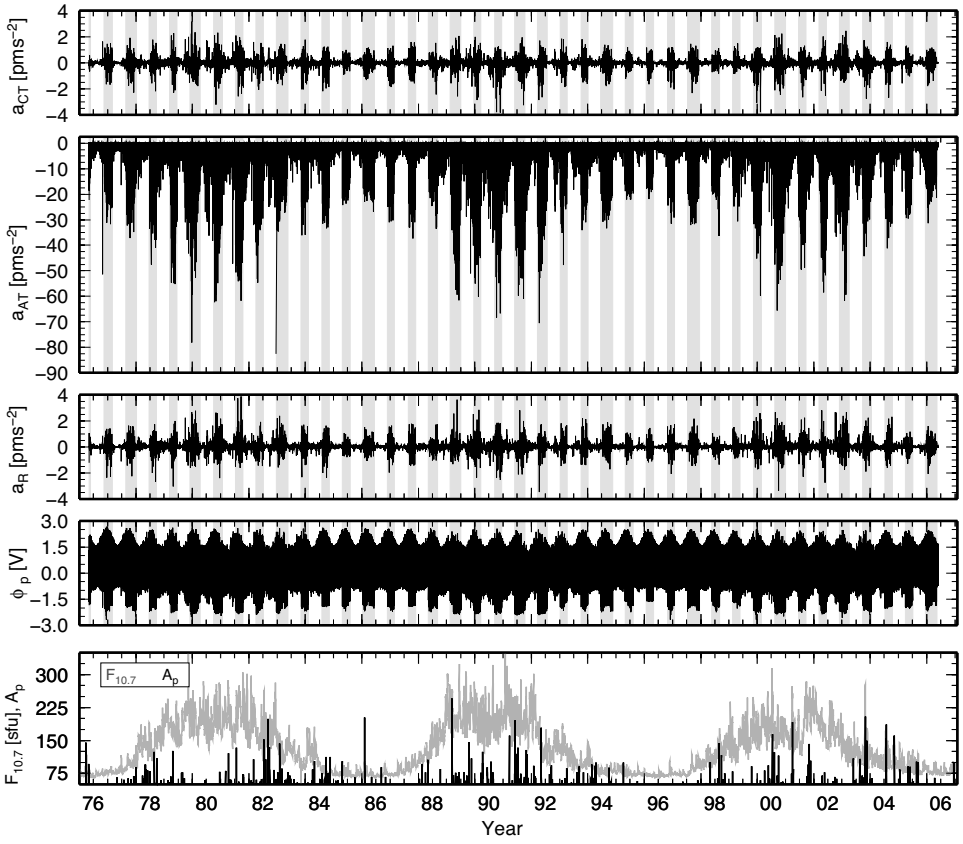

Figure 3: Instantaneous CPD acceleration (cross-track, along-track and radial respectively), satellite potential and activity indices for LAGEOS-I, from launch until June 4, 2006.

together with the small drift of the ion speeds (less than 10% of the orbital speed) given by SCTIP, contribute to yield the aforementioned values.
The same (slightly smaller) modulation can be noticed in the negative values attained by the satellite floating potential for both satellites. The amplitude of the signal is larger for LAGEOS-I than for LAGEOS-II, due to the higher temperatures attained by the first one, *cf.* Equations 7 and 4.

In spite of these figures being suitable for observing temporal variations in the accelerations due to changes in the activity indices through their lifetime, the form of these accelerations and its direct relation to changes in the plasmatic parameters is best depicted when concentrating on a single day, as done in Figures 5 and 6. Said figures represent the instantaneous acceleration components, together with the aforementioned ideal shadow function, the activity indices (now with the 3-hourly a_p index instead of the daily A_p one), the plasmatic parameters for both ions and electrons, and

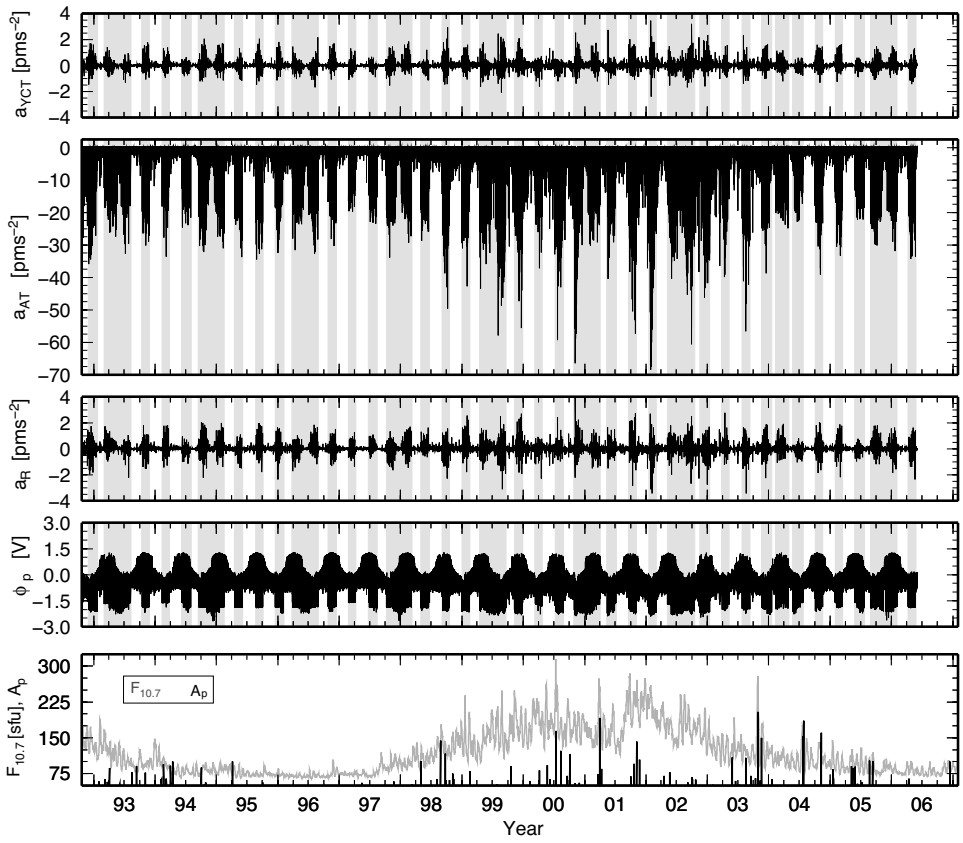

Figure 4: Instantaneous CPD acceleration (cross-track, along-track and radial respectively), satellite potential ϕ, and activity indices for LAGEOS-II, from launch until June 4, 2006.

their product for a chosen date. The selected day for LAGEOS-I is a period withouth eclipse passages and with quiet solar and geomagnetic conditions ($F_{10.7} = 75.1$ sfu and $a_p \in [0, 12]$, *i.e.*, $K_p \in [0\text{o}, 3-]$) on January 1, 1996. As for LAGEOS-II, the selected date (March 1, 2000) corresponds to very high solar activity condictions ($F_{10.7} = 203.2$ sfu) and moderate geomagnetic activity ($a_p \in [6, 22]$, *i.e.*, $K_p \in [2-, 4-]$), combined with shadow passages. Clearly, neither the plasmatic properties n, T nor the floating potential are constant along an orbital revolution, thus contributing to the appearance of spikes in the accelerations along the orbit. It seems that the maxima of temperature and density are in counterphase, leaving the total product quite stable, due to opposite reactions to the energy input. The importance of (combinations of this) product has already been pointed out by *Al'pert* [1990] and *Afonso et al.* [1985]. Deviations from this constant value, together with the associated floating potential variations, result into tangi-

ble acceleration values, in particular when $log(nT) > 13.5$, for this product is proportional to the thermal pressure exerted by the ions (*cf.* Equation 14). It must be noted that the difference between the ion species represented there (H^+) and electron concentrations as given by the SCTIP model is rather high, at least one order of magnitude, which comes into conflict with the quasi neutrality condition of a plasma. For this reason, and following the conservative solution mentioned above, the concentration of the (selected) protons has been put equal to that of the electrons for all the calculations presented here. An immediate comparison between these figures show that the average (negative) values of the along-track acceleration is $\in [1, 5]$ pm s^{-2}, and shows occasional peaks when in eclipse passages of about 15 pm s^{-2} for high solar activity, whereas for normal activity and non-eclipse periods, these (negative) peaks reduce to 6 pm s^{-2} (for this particular date). The average value proposed in literature for this dynamical contributor is approximately $\in [1.8, 4.5]$ pm s^{-2}, with minimum values reported by *Rubincam* [1980], and maximum values provided by *Afonso et al.* [1980] (for a cylinder).

Although the mathematical formulation presented here is more complete than those presented previously, uncertainties have been shown to be large for the polar regions, and in the order of 30% for the temperature for low and mid MLAT. This translates directly into the ion thermal pressure nkT, yet the contribution of the temperature to the problem is more subtle (*e.g.* the floating potential and the dimensionless speed), meaning that any estimation not having both the temperature and concentration uncertainties would be unrealistic. Thus only a crude estimation for the CPD accelerations in the polar regions, subject to higher uncertainties, can be done, leaving an uncertainty of about a 40%. Notwithstanding this, the inequality $log(nT) > 13.5$ occurs when the satellite is in the plasmasphere region, rather than when in the auroral or polar ones. This increases our confidence in the results, since the expected deviations are much smaller in the former region. An interesting feature already mentioned in *Barlier et al.* [1986] is the negative correlation between CPD and CPD, *i.e.*, when the former decreases (high solar activity therefore smaller hydrogen density), the latter increases (higher energy inputs and thus higher temperature values which compensate for the decrease in overall density), yielding a constant contribution, plus a modulation caused by CPD due to variations in the nT product mentioned above.

An additional comment regarding the interpolation procedure in the transitions between plasmasphere and auroral regions, and between auroral and polar regions. Figures 5 and 6 depict the temperature and density for about 6 orbital revolutions. For both LAGEOS, the transition between zones (observed by an increase in the temperature with a corresponding decrease in concentration) is rather smooth and approaching the boundary conditions imposed in Table 2. LAGEOS-II slightly passing through the auroral

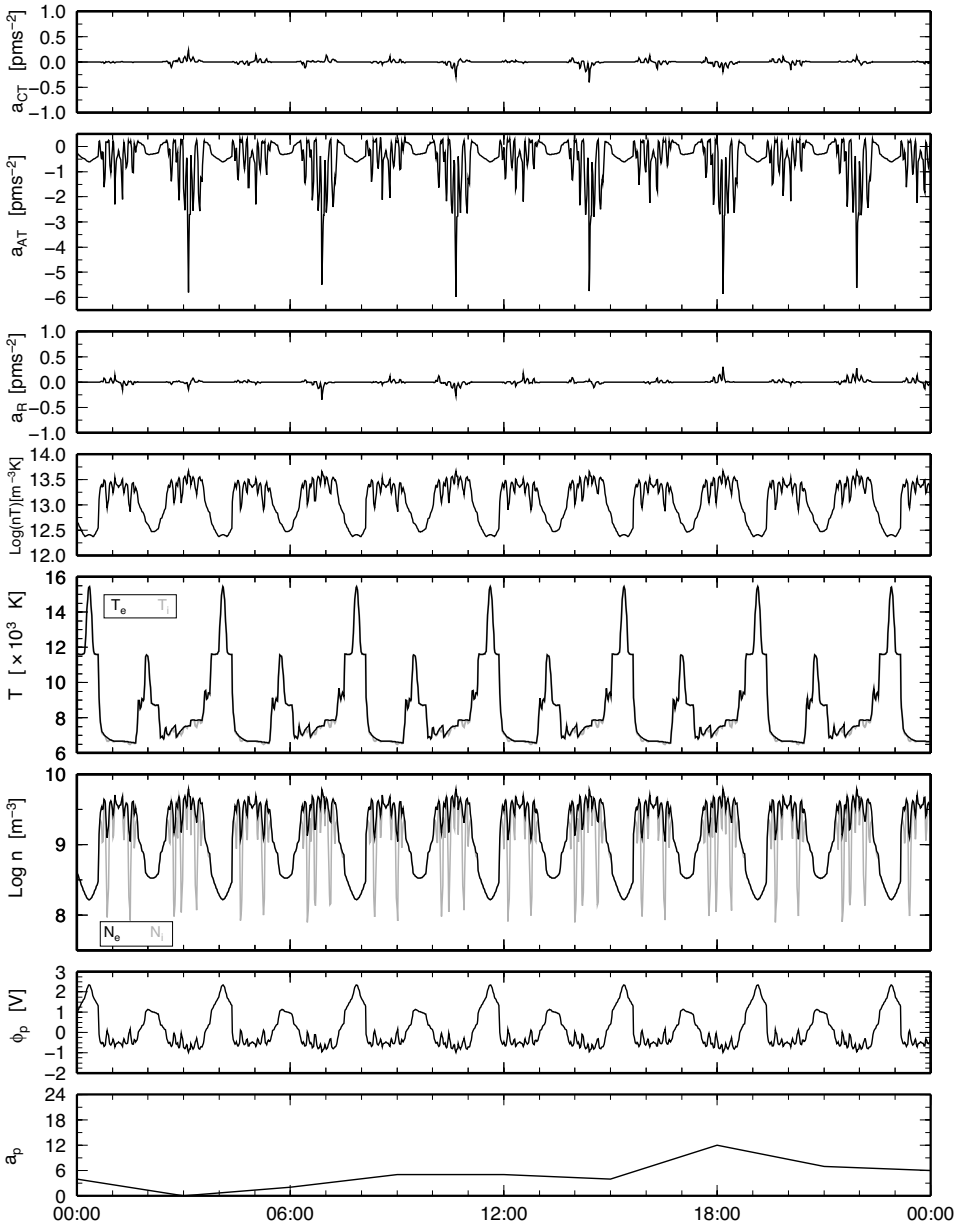

Figure 5: CPD acceleration, plasmatic parameters, floating potential, and geomagnetic activity index a_p simulated over one particular day (January 1, 1996) for LAGEOS-I. The solar activity value on this day corresponds to $F_{10.7} = 75.1$ sfu.

zones result into a minor variation when compared to the steeper profiles obtained for LAGEOS-I.

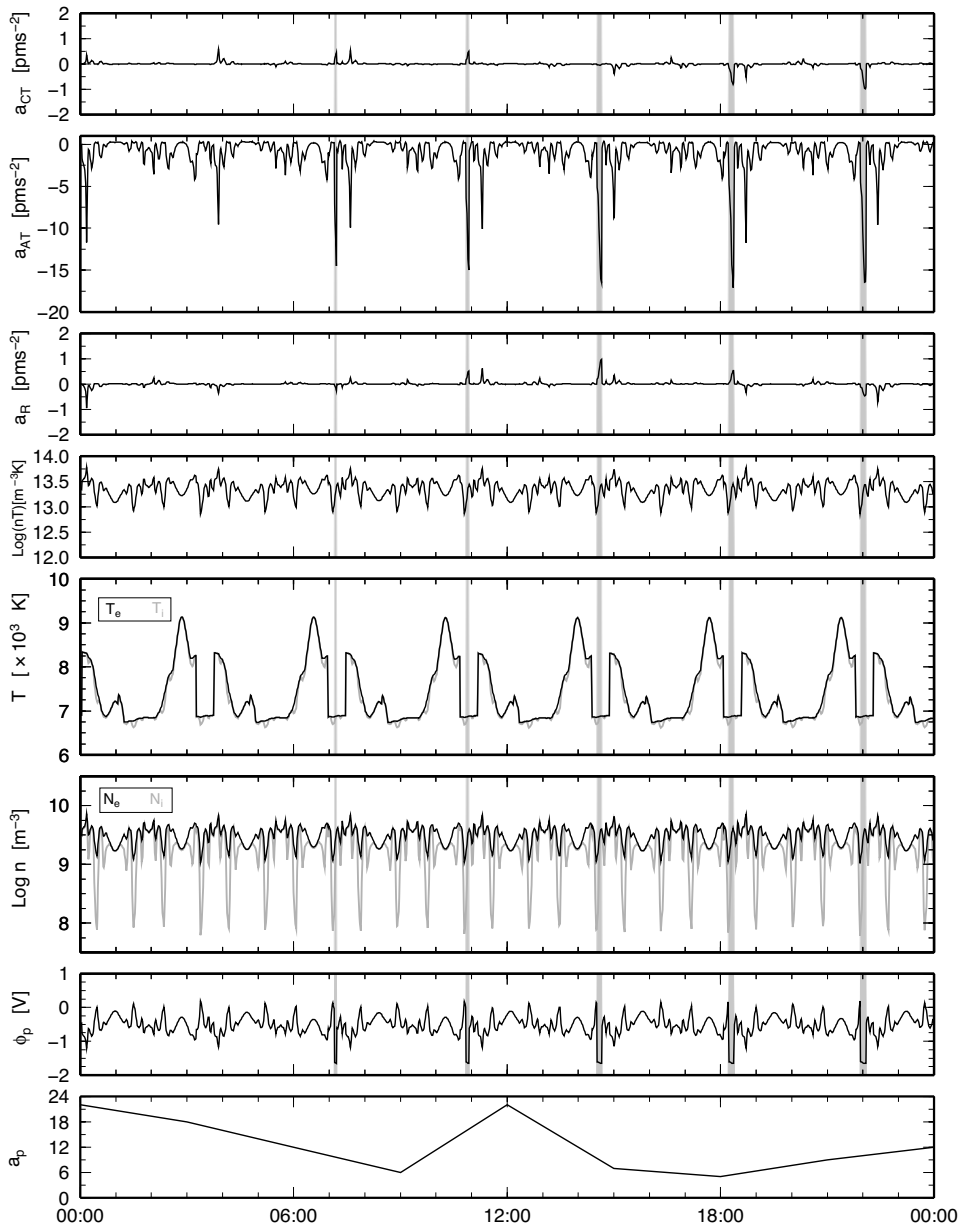

Figure 6: CPD acceleration, plasmatic parameters, floating potential, and geomagnetic activity index a_p simulated over one particular day (March 11, 2000) for LAGEOS-II. The solar activity value on this day corresponds to $F_{10.7} = 203.2$ sfu. Grey bands indicate eclipse passages.

8 Conclusions

Motivated by this new found eclipse dependent contributor, innovative theoretical studies on CPD (more in particular on the scattering contribu-

tion) and implementation of more recent models describing the spatial and temporal behaviour of the plasmasphere, have made possible a proper complete theoretical and numerical analysis of one of the remaining open issues in the LAGEOS non-gravitational perturbations modelling: the CPD with its two constituents, drag due to direct collision and due to scattering of the incoming species. The total expression has been found to be dependent on the ion thermal pressure, a power series of the (dimensionless) floating potential with almost constant coefficients for the entire velocity range studied, and a monotonically increasing function of the dimensionless speed. The dependency of the thermal pressure on several physical parameters (concentration and temperature of the environmental plasma) has been quantified, and the dependency of the plasmatic parameters on solar and geomagnetic activity has been shown to play a major role in the resulting acceleration. The resulting accelerations are modulated by eclipse passages, solar activity, and geomagnetic activity (for large values of the A_p index). When not in eclipse, the CPD values are in the order of a few pms^{-2}, as proposed in previous studies. However, when in eclipse, the amplitudes (of the nominal models) increase up to -85 pms^{-2} and -70 pms^{-2} for LAGEOS-I and LAGEOS-II, respectively. In turn this is due to an increase of the ion thermal pressure for said passages. These larger values for LAGEOS-I than for LAGEOS-II are most likely due to the different orbital configuration, which brings LAGEOS-I over the auroral and polar zones, with higher variations of the plasmatic parameters, and therefore of the spacecraft floating potential and the resulting accelerations. Due to a large uncertainty in the plasmatic parameters (concentration and temperature), up to 30% for low and mid MLAT, the CPD contribution is the most uncertain of all the effects considered here. Considering (global) variations of 30% of the plasmatic parameters, the relative variations in the acceleration amount up to 20% of the the maximum amplitudes presented above. It seems therefore that a more detailed knowledge of these parameters is desirable for any subsequent study.

References

Afonso, G., F. Barlier, C. Berger, and F. Mignard (1980), The effect of atmospheric braking and electric drag on the trajectory of the LAGEOS satellite, *Academie des Science Paris Comptes Rendus Serie B Sciences Physiques*, *290*, 445–448.

Afonso, G., F. Barlier, C. Berger, F. Mignard, and J. J. Walch (1985), Reassessment of the charge and neutral drag of LAGEOS and its geophysical implications, *Journal of Geophysical Research*, *90(B11)*, 9381–9398.

Al'pert, Y. L. (1990), *Space plasma, theory and main properties*, vol. 1, 308, Cambridge Atmospheric and Space Science Series, Cambridge University Press, New York, NY, USA.

Andres, J. I. (2007), *Enhanced Modelling of LAGEOS Non-Ggravitational Perturbations*,

Ph.D. dissertation, Delft Institute for Earth Observation and Space Systems, Delft University of Technology, Delft, The Netherlands.

Andrés, J. I., R. Noomen, and S. Vecellio None (2006), Numerical simulation of LAGEOS thermal behaviour and thermal accelerations, *Journal of Geophysical Research*, *111*, *B09406*, doi:10.1029/2005JB003928.

Barlier, F., M. Carpino, P. Farinella, F. Mignard, A. Milani, and A.M. Nobili (1986), Non-gravitational perturbations on the semimajor axis of LAGEOS, *Annales Geophysicae*, *4(A)*, 193 – 210.

Brundin, C. L. (1963), Effects of charged particles on the motion of an earth satellite, *AIAA Journal*, *1*(11), 2529–2538.

Comfort, R. H. (1996), Thermal structure of the plasmasphere, *Advances in Space Research*, *17*, 175–184.

Daugherty, J. E., R. K. Porteous, M. D. Kilgore, and D. B. Graves (1992), Sheath structure around particles in low-pressure discharges, *Journal of Applied Physics*, *72*(9), 3934–3942.

Fournier, G. (1971), *Thèse de Doctorat d'État*, Ph.D. dissertation, Faculté des Sciences d'Orsay, Orsay, France.

Ganguli, G., M. A. Reynolds, and M. W. Liemohn (2000), The plasmasphere and advances in plasmaspheric research, *Journal of Atmospheric and Solar-Terrestrial physics*, *62*, 1647–1657.

Hutchinson, I. H. (1987), *Principles of plasma diagnostics*, 379, Cambridge University Press, New York, NY, USA.

Hutchinson, I. H. (2002), Ion collection by a sphere in a flowing plasma: 1. Quasineutral, *Plasma Physics and Controlled Fusion*, *44*, 1953–1977, doi:10.1088/0741-3335/44/9/313.

Hutchinson, I. H. (2003), Ion collection by a sphere in a flowing plasma: 2. Non-zero Debye length, *Plasma Physics and Controlled Fusion*, *45*, 1477–1500, doi:10.1088/0741-3335/45/8/307.

Hutchinson, I. H. (2005), Ion collection by a sphere in a flowing plasma: 3. Floating potential and drag force, *Plasma Physics and Controlled Fusion*, *47*, 71–87, doi:10.1088/0741-3335/47/1/005.

Hutchinson, I. H. (2006), Collisionless ion drag force on a spherical grain, *Plasma Physics and Controlled Fusion*, *47*, 185–202, doi:10.1088/0741-3335/48/2/002.

Johnson, M. T., J. R. Wygant, C. A. Cattell, F. S. Mozer, M. Temerin, and J. Scudder (2001), Observations of the seasonal dependence of the thermal plasma density in the Southern Hemisphere auroral zone and polar cap at 1R, *Journal of Geophysical Research*, *106*, 19023–19034, sep 2001, doi: 10.1029/2000JA900147.

Khrapak, S. A., A. V. Ivlev, G. E. Morfill, and H. M. Thomas (2002), Ion drag force in complex plasmas, *Physical Review E*, *66*, 046414(4), doi:10.1103/PhysRevE.66.046414.

Kletzing, C. A., F. S. Mozer, and R. B. Torbert (1998), Electron temperature and density at high latitude, *Journal of Geophysical Research*, *103*, 14837–14845.

Laframboise, J. G. (1966), Theory of spherical and cylindrical Langmuir probes in a collisionless Maxwellian plasma at rest, *UTIAS Technical Report 100*, University of Toronto, Institute for Aerospace Studies, Toronto, Canada.

Lam, S. H. (1965), Unufied Theory for the Langmuir Probe in a Collisionless Plasma, *Physics of Fluids*, *8*, 73–87.

McIlwain, C. E. (1961), Coordinates for mapping the distribution of magnetically trapped particles, *Journal of Geophysical Research*, pp. 3681–3691.

Millward, G. H., R. J. MoAett, S. Quegan, and T. J. Fuller-Rowell (1996), A coupled thermosphere-ionosphere-plasmasphere model CTIP, in *Solar Terrestrial Energy Program, Handbook of Ionospheric Models*, edited by R. W. Schunk, pp. 239–280, Scientific COmmittee on Solar Terrestrial Physics (SCOSTEP).

Nsumei, P. A., X. Huang, B. W. Reinisch, P. Song, V. M. Vasyliunas, J. L. Green, S. F. Fung, R. F. Benson, and D. L. Gallagher (2003), Electron density distribution over the northern polar region deduced from IMAGE/radio plasma imager sounding, *Journal of Geophysical Research (Space Physics)*, *108*, 11, feb 2003, doi: 10.1029/2002JA009616.

Pitts, W. C., and E. D. Knechtel (1965), Experimental investigation of electrical drag on spherical satellite models, *NASA Technical Note TN D–2619*, NASA.

Rubincam, D. P. (1980), On the Secular Decrease in the Semimajor Axis of LAGEOS' Orbit, *NASA Technical Memorandum TM 80734*, NASA.

Rubincam, D. P. (1990), Drag on the LAGEOS satellite, *Journal of Geophysical Research*, *95(B4)*, 4881–4886.

Smith, D. E., and P. J. Dunn (1980), Long term evolution of the LAGEOS orbit, *Geophysical Research Letters*, *7*, 437–440.

Tu, J., P. Song, B. W. Reinisch, X. Huang, J. L. Green, H. U. Frey, and P. H. Reiff (2005), Electron density images of the middle- and high-latitude magnetosphere in response to the solar wind, *Journal of Geophysical Research*, *110*(A12210), 12 pp., doi: 10.1029/2005JA011328.

Uglov, A. A., and A. G. Gnedovets (1991), Effect of particle charging on momentum and heat transfer from rarefied plasma flow, *Plasma Chemistry and Plasma Processing*, *11*(2), 251–267, doi:10.1007/BF01447245.

Watson, D. F. (1982), Acord: Automatic contouring of raw data, *Computers and Geosciences*, *1 (8)*, 97–101.

◄ BACK TO SESSION DETAILED CONTENTS ◄ BACK TO HIGHER-LEVEL CONTENTS